

Sensitivity of the interlayer magnetoresistance of layered metals to intralayer anisotropies

Malcolm P. Kennett¹ and Ross H. McKenzie²

¹ *Physics Department, Simon Fraser University,*

8888 University Drive, Burnaby, British Columbia, V5A 1S6, Canada

² *Physics Department, University of Queensland, Brisbane 4072, Australia*

(Dated: March 23, 2022)

Many of the most interesting and technologically important electronic materials discovered in the past two decades have both a layered crystal structure and strong interactions between electrons. Two fundamental questions about such layered metals concern the origin of intralayer anisotropies and the coherence of interlayer charge transport. We show that angle dependent magnetoresistance oscillations (AMRO) are sensitive to anisotropies around an intralayer Fermi surface and can hence be a complementary probe of such anisotropies to angle-resolved photoemission spectroscopy (ARPES) and scanning tunneling microscopy (STM). However, AMRO are not very sensitive to the coherence of the interlayer transport which has implications for recent AMRO experiments on an overdoped cuprate.

PACS numbers: 71.18.+y, 72.10.-d, 74.72.-h, 74.70.Kn

I. INTRODUCTION

For elemental metals, such as tin and sodium, it is well established that a Fermi liquid description is valid. Thus the Bloch wavevector is a good quantum number for electronic excitations and there is a well-defined three-dimensional Fermi surface (FS).¹ Any variation of properties over the FS is of secondary interest. In contrast, many layered metals (e.g., cuprates and layered manganites) are distinctly different. Their properties cannot be described in terms of a Fermi liquid picture.² Even when one sees signatures of an intralayer FS, suggesting quantum coherence of excitations within individual layers, there is controversy over what length and time scales the electronic excitations are coherent between layers.³ Furthermore, in the cuprates properties such as the pseudogap, the quasiparticle spectral weight, and scattering rate, vary significantly over the intralayer FS.² These variations, also seen in ARPES⁴ and STM⁵ may be key to understanding the origin of the superconductivity and the unusual properties of the metallic and pseudogap phases.² Significant anisotropies in quasiparticle weight were also seen recently in layered manganites.⁶ We show here how the dependence of the interlayer magnetoresistance on the the magnetic field orientation is quite sensitive to intralayer anisotropies.

Angle dependent magnetoresistance oscillations (AMRO). The dependence of the interlayer magnetoresistance on the magnetic field direction has been used to map out a three-dimensional (3d) FS in a chemically diverse range of layered metals. including organic charge transfer salts,^{7,8} ruthenates,^{9,10} semiconductor heterostructures,¹¹ tungsten bronzes,¹² intercalated graphite,¹³ and an overdoped thallium cuprate.^{14,15} However, most of the observed AMRO are also consistent with a a two-dimensional FS, i.e., a FS existing only within the individual layers and weakly incoherent interlayer transport.¹⁶ Hence, it is difficult

to experimentally distinguish the two physically distinct pictures summarised in Fig. 1.¹⁶ AMRO are essentially a geometric resonance involving the cyclotron orbits projected onto the plane parallel to the layers.¹⁷ In this sense they are similar to geometric commensurability oscillations in magnetoresistance seen for two dimensional electron gases in semiconductor heterostructures.^{18,19,20}

In this paper we present the following new results for interlayer magnetotransport in a layered Fermi liquid metal. (i) We give a general expression for the interlayer conductivity in a tilted magnetic field including the effects of anisotropy around the FS of the Fermi wave vector, Fermi velocity, scattering rate, quasiparticle weight, and interlayer hopping integral. (ii) We derive (i) for both coherent interlayer transport (a three-dimensional FS) and for weakly incoherent interlayer transport (where the FS is only well defined within the layers). [See Fig. 1]. Furthermore, we elucidate the physics behind why the same result is obtained for both types of interlayer transport.²¹ (iii) Our results show that a three-dimensional FS is *not necessary* to give a quantitative description of AMRO experiments on an overdoped cuprate.¹⁴ The data can be reproduced by the weakly incoherent model. Others have considered the effect on AMRO of various specific anisotropies and specific field directions,^{7,10,22,23} but not the general case considered here.

The paper is structured as follows. In Sec. II we introduce the anisotropies in FS properties that we consider and state our main result, Eq. (9) for interlayer conductivity in the presence of these anisotropies. In Sec. III we discuss the derivation of our main result for the interlayer conductivity for both coherent and weakly incoherent interlayer transport. In Sec. IV we explore the implications of these results for AMRO experiments on thallium cuprate.¹⁴ Finally, in Sec. V we conclude and give a discussion of our results.

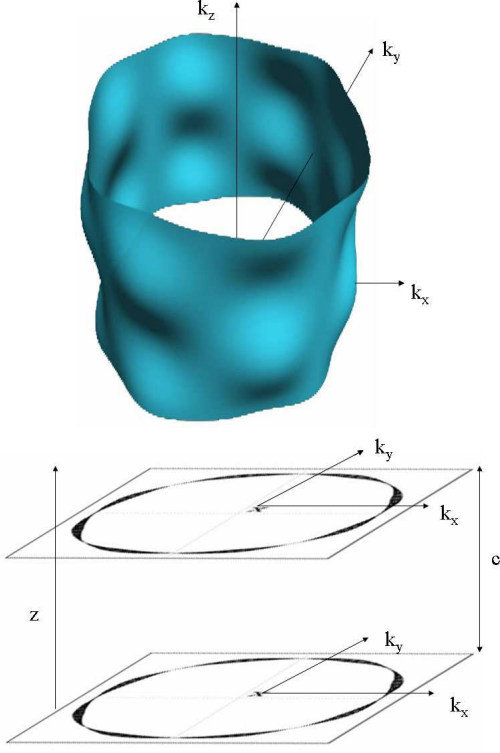


FIG. 1: Two pictures of interlayer transport. (i) The Fermi surface (FS) is three dimensional and warped by the quantum coherence of electron transport between layers and the variation of the interlayer hopping with the intralayer wavevector.^{10,14} (ii) The FS is only well defined within individual layers. The interlayer transport is weakly incoherent, i.e. momentum parallel to the layers is conserved but coherence is only between neighbouring layers. The thickness of the line is proportional to the magnitude of the interlayer hopping.

II. ANISOTROPIES IN THE FERMI SURFACE AND TRANSPORT

There are a number of FS properties that can be anisotropic in layered metals. We discuss intralayer anisotropy in the Fermi surface, dispersion and in-plane scattering, and anisotropy in the interlayer hopping. All these anisotropies have been considered in earlier works, but not simultaneously, which is the generic situation.

We will consider the interlayer conductivity in a tilted magnetic field,

$$\mathbf{B} = B(\sin \theta \cos \varphi, \sin \theta \sin \varphi, \cos \theta), \quad (1)$$

which is at an angle θ to the c -axis and makes an azimuthal angle φ to the a -axis in the ab plane (see inset to Fig. 2).

A. Intralayer anisotropies.

We use the angle ϕ to parametrize the intralayer FS defined by

$$\mathbf{k}_F(\phi) = k_F(\phi)(\sin \phi, \cos \phi). \quad (2)$$

For an anisotropic in-plane dispersion, $\epsilon_{2d}(k_x, k_y)$, the Fermi wavevector \mathbf{k}_F , which maps out a surface (strictly speaking, a curve) of constant energy surface, and is defined by $\epsilon_{2d}(\mathbf{k}_F(\phi)) = E_F$, where E_F is the Fermi energy. The Fermi velocity is defined by,

$$\mathbf{v}_F(\phi) = \frac{1}{\hbar} \frac{\partial \epsilon}{\partial \mathbf{k}} \Big|_{\mathbf{k}=\mathbf{k}_F} \quad (3)$$

and is always normal to the Fermi surface. Hence, if there is intralayer anisotropy in the dispersion relation there must also be anisotropy in *both* the Fermi surface and Fermi velocity.

Cyclotron frequency. The semi-classical equations of motion¹ for an electron moving on the intralayer FS in a magnetic field with component $B \cos \theta$ perpendicular to the layers can be solved give the variation of the angular speed due to cyclotron motion around the intralayer FS as

$$\omega_0(\phi) = eB \cos \theta \frac{\mathbf{k}_F(\phi) \cdot \mathbf{v}_F(\phi)}{\hbar k_F(\phi)^2}, \quad (4)$$

where $\mathbf{v}_F(\phi)$ is the Fermi velocity. For a circular FS $\omega_0(\phi)$ has a constant value, $\omega_c \cos \theta$, with $\omega_c = eB/m^*$, the cyclotron frequency. However, for an anisotropic FS, \mathbf{k}_F and \mathbf{v}_F are not parallel and $\omega_0(\phi)$ will vary around the FS.

Scattering rate. The variation of the transport lifetime over the FS is given by $\tau(\phi)$. The probability of an electron not being scattered in moving between two points on the intralayer FS, defined by angles ϕ_2 and ϕ_1 , is

$$G(\phi_2, \phi_1) = \exp \left(- \int_{\phi_1}^{\phi_2} \frac{d\psi}{\omega_0(\psi)\tau(\psi)} \right). \quad (5)$$

In what follows an important quantity is $P \equiv G(2\pi, 0)$, the probability that an electron makes a complete orbit of the intralayer FS without being scattered.

Interlayer hopping. The Hamiltonian for hopping between the layers is:

$$\mathcal{H}_\perp = \sum_{ij} t_\perp(\mathbf{r}_i - \mathbf{r}_j) \left[c_i^\dagger c_j e^{i\Phi_{ij}} + c_j^\dagger c_i e^{-i\Phi_{ij}} \right], \quad (6)$$

where $\Phi_{ij} = (ec/\hbar)(A_z(\mathbf{r}_i) - A_z(\mathbf{r}_j))$ is the Aharonov-Bohm (AB) phase acquired by an electron hopping between \mathbf{r}_i in one layer and \mathbf{r}_j in the other layer,¹⁷ with layer separation c and $\mathbf{A}_\parallel = A_z(\mathbf{r})\hat{\mathbf{z}} = \frac{1}{2}(\mathbf{B}_\parallel \times \mathbf{r})$ the vector potential for the magnetic field parallel to the layers, \mathbf{B}_\parallel . Momentum anisotropy in t_\perp is present in the Fourier transform of the hopping matrix element $t_\perp(\mathbf{r}_i - \mathbf{r}_j)$ via

$$t_\perp(\phi) = \int d^2\mathbf{r} \exp(i\mathbf{k}_F(\phi) \cdot \mathbf{r}) t_\perp(\mathbf{r}). \quad (7)$$

In momentum space the difference in AB phases acquired in hopping between layers for positions ϕ_1 and ϕ_2 on the FS is

$$\Phi(\phi_2, \phi_1) = c \tan \theta [k_F(\phi_1) \cos(\phi_1 - \varphi) - k_F(\phi_2) \cos(\phi_2 - \varphi)]. \quad (8)$$

We will also see that for a coherent three-dimensional FS this quantity can be related to the Bloch wavevector perpendicular to the layers (cf. Eq. (15) below).

B. The main result

We now state a new result, central to this paper. The interlayer conductivity, σ_c in a tilted magnetic field, [Eq. (1)] at zero temperature is

$$\sigma_c(\theta, \varphi) = \frac{s_0 e B \cos(\theta)}{(1-P)} \int_0^{2\pi} \frac{d\phi_2}{\omega_0(\phi_2)} \int_{\phi_2-2\pi}^{\phi_2} \frac{d\phi_1}{\omega_0(\phi_1)} \times t_{\perp}(\phi_2) t_{\perp}(\phi_1) \cos(\Phi(\phi_1, \phi_2)) G(\phi_2, \phi_1), \quad (9)$$

where $s_0 = (e^2 c / \pi^2 \hbar^4)$. The factor $1/(1-P)$ in the conductivity comes from noting the 2π periodicity of the integrand and reducing the integration region for ϕ_1 . The factor $eB \cos \theta / \omega_0(\phi_2)$ can also be interpreted as anisotropy in the density of states.²³ Equation (9) does not explicitly take into account possible anisotropy in the quasiparticle weight $Z(\phi)$, due to many-body effects. The hopping matrix elements $t_{\perp}(\phi)$ should be understood as $t_{\perp}(\phi) = Z(\phi) t_{\perp}^0(\phi)$, where $t_{\perp}^0(\phi)$ is the bare hopping. It should be stressed that Eq. (9) depends *only* on *intralayer* FS properties, and holds irrespective of the particular form of those anisotropies.

In Sec. III we give the derivation of this result for both coherent transport perpendicular to the layers and for weakly incoherent interlayer hopping (see Fig. 1), provided $t_{\perp} \ll E_F$. Below, in Fig. 2 we show the calculated AMRO for parameters that fit the experimental data for the overdoped thallium cuprate in Ref. 14. The fitting procedure in Ref. 14 allowed for anisotropy in the FS, but not in the Fermi velocity (i.e., in $\omega_0(\phi)$) or in the intralayer scattering. Allowing for both of these factors we find a very high quality, quantitative fit to the data, which for clarity of presentation is not shown, since it lies virtually on top of our calculated magnetoresistance.

C. Mapping out Fermi surface anisotropies at high magnetic fields

We now consider AMRO in high magnetic fields ($\omega_{00}\tau_0 \gg 1$), since such experiments have previously been used to map out the FS for very clean organic materials.^{7,8,24} When $ck_F \tan \theta \gg 1$ and $cv_F \tau_0 eB / \hbar^2 \gg 1$ the method of steepest descents may be used to evaluate the integrals in Eq. (9).²⁵ The integrals are dominated by

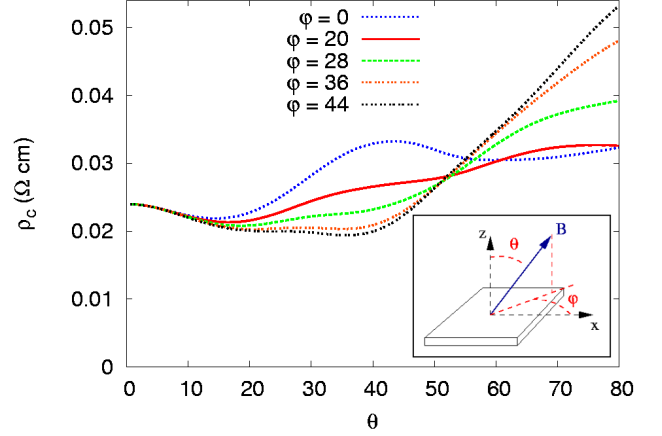


FIG. 2: Calculated angular dependence of the interlayer resistance for several different azimuthal angles. The parameters are chosen (see Sec. IV for precise parametrization) so that the calculated curves agree essentially perfectly with the measured curves for the overdoped cuprate Tl2201.¹⁴ The inset shows the direction of the magnetic field relative to the layers of the crystal.

the angles near ϕ_0 which is where the Fermi wavevector, $k_F(\phi)$ has the maximum projection along the direction of the intralayer magnetic field, $\mathbf{b}_{\parallel} \equiv (\cos \varphi, \sin \varphi)$. ϕ_0 is a φ dependent quantity and is found from the solution of

$$\frac{\partial}{\partial \phi} (\mathbf{b}_{\parallel}(\varphi) \cdot \mathbf{k}_F(\phi)) = 0.$$

This leads to

$$\sigma_c(\theta, \varphi) \simeq \frac{2\pi s_0}{(1-P)} \frac{t_{\perp}(\phi_0)^2}{(\omega_0(\phi_0))^2} \frac{eB \cos \theta}{|\mu(\phi_0)| c \tan \theta} \times \left[1 + 2P^{\frac{1}{2}} \sin(2c \tan \theta \mathbf{b}_{\parallel}(\varphi) \cdot \mathbf{k}_F(\phi_0)) \right], \quad (10)$$

where $\mu(\phi) = \frac{\partial^2}{\partial \phi^2} [\mathbf{b}_{\parallel}(\varphi) \cdot \mathbf{k}_F(\phi)]$. This expression shows that the interlayer magnetoresistance oscillates as a function of the field tilt angle and for a fixed value of φ the magnetoresistance will be a maximum when the field is at angles θ_n given by^{7,24,25}

$$\mathbf{b}_{\parallel}(\varphi) \cdot \mathbf{k}_F(\phi_0) c \tan \theta_n = \pi(n - 1/4) \quad (11)$$

where $n = 1, 2, \dots$. This expression has been used to map out the intralayer FS for a wide range of metallic organic charge transfer salts.^{7,24} We point out that our expression (10) will also be sensitive to angular variations in the interlayer hopping and cyclotron frequency. Interestingly, when $\omega_{00}\tau_0 \gg 1$ there is no ϕ_0 dependence from the angular variation in the scattering rate since the only dependence on the scattering rate is through the quantity P , which involves an average over the FS. Hence, the FS shape may be determined independently of scattering, which can then be used to determine the anisotropy in scattering at smaller fields.²⁶

III. DERIVATIONS FOR COHERENT AND INCOHERENT INTERLAYER TRANSPORT

We now sketch the derivation of Eq. (9) for the cases of coherent and weakly incoherent interlayer transport.

A. Coherent interlayer transport.

If $t_\perp \gg \hbar/\tau$, then there is a well-defined Bloch wavevector perpendicular to the layers, k_z and the three-dimensional dispersion is

$$\mathcal{E}_{3d} = \mathcal{E}_{2d}(k_x, k_y) - 2t_\perp^0(k_x, k_y) \cos(ck_z). \quad (12)$$

To obtain Eq. (9) within a picture of coherent interlayer transport one starts from the dispersion, which can be used to determine the Fermi velocity, and semi-classical equations of motion for motion on the FS. Solution of the appropriate Boltzmann equation, to leading order in $(t_\perp/E_F)^2$, leads to Eq. (9) as a generalization of the Shockley-Chamber's (SC) formula.^{1,27}

A useful relation between the projection of the motion in real space onto the plane of the layers and c -axis momentum (where \mathbf{R}_\parallel is the position in the plane) comes from considering the equation of motion (we neglect higher order terms in t_\perp/E_F). Integrating to get in-plane and c -axis momentum gives

$$\mathbf{k}_\parallel(t) = \mathbf{k}_\parallel(0) + \frac{eB_\perp}{\hbar} [\mathbf{R}_\parallel(t) - \mathbf{R}_\parallel(0)] \times \hat{\mathbf{z}}, \quad (13)$$

$$k_z(t) = k_z(0) + \frac{\mathbf{B}_\parallel \cdot (\mathbf{k}_\parallel(t) - \mathbf{k}_\parallel(0))}{B_\perp}. \quad (14)$$

Hence, the interlayer velocity is

$$v_z(\phi) = \frac{2ct_\perp^0(\phi)}{\hbar} \sin(ck_z(0) + ck_F(\phi) \tan \theta \cos(\phi - \varphi)). \quad (15)$$

The SC formula¹ involves correlations in this velocity at different times (equivalently different ϕ)

$$\begin{aligned} \sigma &= \frac{e^2}{4\pi^3} \int d^3\mathbf{k}_1 v_z(\mathbf{k}_1) \left(-\frac{\partial f_T}{\partial \epsilon} \right) \\ &\times \int_{-\infty}^{\phi_1} d\phi_2 \frac{v_z(\phi_2)}{\omega_2(\phi_2)} G(\phi_2, \phi_1), \end{aligned} \quad (16)$$

where $G(\phi_2, \phi_1)$ was defined in Eq. (5), f_T is the Fermi-Dirac distribution, and the limits of integration for k_z are between $\pm \frac{\pi}{c}$. The expressions in Eqs. (13)-(15) (when the integral over k_z is performed in Eq. (16)) allow us to see how the term associated with an Aharonov-Bohm phase for weakly incoherent transport (c.f., Eq. (8)) arises for coherent interlayer transport.¹⁷

B. Weakly incoherent interlayer transport.

The interlayer current at \mathbf{r}_1 from layer 2 is²⁸

$$j_\perp(\mathbf{r}_1) = ie \int d^2\mathbf{r}_2 t_\perp(\mathbf{r}_1 - \mathbf{r}_2) \left[c_2^\dagger(\mathbf{r}_2) c_1(\mathbf{r}_1) e^{i\Phi_{12}} - h.c. \right],$$

where Φ_{12} is the gauge phase for hopping between the layers. Note that $t_\perp(\mathbf{r}_1, \mathbf{r}_2)$ contains the variation of the interlayer hopping over the FS [Eq. (7)].

In linear response the Kubo formula for the interlayer conductivity at zero temperature is^{16,28}

$$\begin{aligned} \sigma_c &= \frac{2ce^2}{\hbar L_x L_y} \text{Re} \left[\int d^2\mathbf{r}_1 \int d^2\mathbf{r}_2 \int d^2\mathbf{r}_3 \int d^2\mathbf{r}_4 \right. \\ &\quad \left. \times t_\perp(\mathbf{r}_1, \mathbf{r}_4) t_\perp(\mathbf{r}_3, \mathbf{r}_2) e^{i(\Phi_{12} - \Phi_{34})} K_{EF}(\mathbf{r}_1, \mathbf{r}_2, \mathbf{r}_3, \mathbf{r}_4) \right], \end{aligned} \quad (17)$$

where²⁹ $K_\epsilon(\mathbf{r}_1, \mathbf{r}_2, \mathbf{r}_3, \mathbf{r}_4) = G_{2,\epsilon}^R(\mathbf{r}_1, \mathbf{r}_2) G_{1,\epsilon}^A(\mathbf{r}_3, \mathbf{r}_4)$ and $G_{1,\epsilon}^R$ is the retarded one-electron Green's function within layer 1. Now, K_ϵ oscillates rapidly as a function of the spatial co-ordinates, with a period comparable to the Fermi wavelength. We can separate the non-oscillatory part by introducing co-ordinates $\mathbf{R}_1 = \frac{1}{2}(\mathbf{r}_1 + \mathbf{r}_4)$, and $\mathbf{R}_2 = \frac{1}{2}(\mathbf{r}_2 + \mathbf{r}_3)$ and write

$$\begin{aligned} K_\epsilon(\mathbf{r}_1, \mathbf{r}_2, \mathbf{r}_3, \mathbf{r}_4) &= \int \frac{d^2\mathbf{k}_1}{(2\pi)^2} \int \frac{d^2\mathbf{k}_2}{(2\pi)^2} K_\epsilon(\mathbf{k}_1, \mathbf{R}_1; \mathbf{k}_2, \mathbf{R}_2) \\ &\times e^{i\mathbf{k}_1 \cdot (\mathbf{r}_1 - \mathbf{r}_4) + i\mathbf{k}_2 \cdot (\mathbf{r}_3 - \mathbf{r}_2)}. \end{aligned} \quad (18)$$

We use a semi-classical approximation since K_ϵ will be sharply peaked at energies around the Fermi energy, which enforces the condition that the magnitude of the momentum in the Fourier transform is ϕ -dependent and lies on the FS and then $K_\epsilon(\mathbf{k}_F(\phi_1), \mathbf{R}_1; \mathbf{k}_F(\phi_2), \mathbf{R}_2)$ satisfies the Boltzmann-type equation for a diffuson:²⁹

$$\begin{aligned} \left[\mathbf{v}_F(\phi_2) \cdot \frac{\partial}{\partial \mathbf{R}_2} + \omega_0(\phi_2) \frac{\partial}{\partial \phi_2} - \frac{1}{\tau(\phi_2)} \right] K_{EF}(\phi_1, \mathbf{R}_1; \phi_2, \mathbf{R}_2) \\ = 2\pi \frac{\omega_0(\phi_1)}{eB \cos \theta} \delta(\phi_1 - \phi_2) \delta(\mathbf{R}_1 - \mathbf{R}_2), \end{aligned}$$

where the factor of ω_0 on the right hand side of the equation comes from noting that the Boltzmann equation is initially stated with $\delta^2(\mathbf{k}_1 - \mathbf{k}_2)$ on the right hand side. We can solve this equation for K by Fourier transforming to get a solution in terms of

$$K(\phi_1, \mathbf{R}_1; \phi_2, \mathbf{q}) = \int \frac{d^2\mathbf{q}}{(2\pi)^2} e^{i\mathbf{q} \cdot \mathbf{R}_2} K(\phi_1, \mathbf{R}_1; \phi_2, \mathbf{R}_2), \quad (19)$$

and then

$$\begin{aligned} K(\phi_1, \mathbf{R}_1; \phi_2, \mathbf{q}) &= 2\pi e^{-i\mathbf{q} \cdot \mathbf{R}_1} \int_{-\infty}^{\phi_2} d\tilde{\phi} \frac{\delta(\phi_1 - \tilde{\phi})}{\omega_0(\tilde{\phi})} \frac{\omega_0(\phi_1)}{eB \cos \theta} \\ &\times e^{-\int_{\phi_2}^{\tilde{\phi}} \frac{d\psi}{\omega_0(\psi)\tau(\psi)}} e^{i\mathbf{q} \cdot \int_{\phi_2}^{\tilde{\phi}} \frac{\mathbf{v}_F(\psi)}{\omega_0(\psi)} d\psi}, \end{aligned} \quad (20)$$

where we can note that

$$\int_{\phi_2}^{\tilde{\phi}} \frac{\mathbf{v}_F(\psi)}{\omega_0(\psi)} d\psi = \mathbf{R}_{\parallel}(\phi_2) - \mathbf{R}_{\parallel}(\tilde{\phi}).$$

Inserting this solution in Eq. (17), using Eq. (13) and integrating over \mathbf{R}_1 and \mathbf{R}_2 forces

$$\Phi = \Phi_{12} - \Phi_{34} = c \tan \theta (k_F(\phi_2) \cos(\phi_2 - \varphi) - k_F(\phi_1) \cos(\phi_1 - \varphi)).$$

so we get as our final result

$$\begin{aligned} \sigma_c = & \frac{2ce^2}{\hbar L_x L_y} \text{Re} \int_0^{2\pi} d\phi_2 \int_{-\infty}^{\phi_2} d\phi_1 \int d\mathbf{R}_1 \int d\mathbf{R}_2 \frac{eB \cos \theta}{\omega_0(\phi_1)} \\ & \times \frac{eB \cos \theta}{\omega_0(\phi_2)} t_{\perp}(\phi_1) t_{\perp}(\phi_2) \cos[\Phi] K_{\epsilon}(\phi_1, \mathbf{R}_1; \phi_2, \mathbf{R}_2), \end{aligned} \quad (21)$$

which is identical to the equation found with the Boltzmann equation for coherent transport in Eq. (9) after using periodicity of the integrand to reduce the interval of integration over ϕ_1 to have length 2π .

IV. AMRO IN THALLIUM CUPRATES

In Secs. II and III we established Eq. (9) for general forms of anisotropy and interlayer transport mechanisms. To illustrate the use of Eq. (9) and its significance we fit recent AMRO measurements of a thallium cuprate.^{14,15} An important point to note about these experiments is that the data is very high quality and it is thus possible to fit AMRO to very high precision, which leads to extraction of FS parameters to high accuracy.

Numerical evaluation of Eq. (9) shows that changing the functional forms of the anisotropy in interlayer hopping and intralayer scattering leads to quantitative variations in the AMRO. This can be seen in Figs. 3 a-c as we add in anisotropies to our fitting of AMRO. To extract deviations of the FS from circularity in a self-consistent manner from AMRO experiments one must also take into account the related anisotropy in the Fermi velocity and the resulting anisotropy in the angular speed (c.f., Eq. (4)). In previous work,^{10,14} such effects were not included in the expressions used for fitting experimental data. This omission quantitatively changes the magnitude of anisotropies in k_F extracted from the fits. Similarly, a self-consistent determination of anisotropy in $\tau(\phi)$ also requires including anisotropy in $\omega_0(\phi)$.

Model forms for anisotropy in thallium cuprates

We use a form of $t_{\perp}(\phi)$ which is consistent with the body-centred-tetragonal crystal structure of thallium cuprate and band structure calculations.^{14,30}

$$t_{\perp}(\phi) = t_{\perp}(\sin(2\phi) + \eta_1 \sin(6\phi) + \eta_2 \sin(10\phi)), \quad (22)$$

parametrized by η_1 and η_2 . The crystal symmetry requires that¹⁰ $t_{\perp}(\phi) = -t_{\perp}(\phi + \pi/2)$, implying $\eta_1 = 1 + \eta_2$, and that $t_{\perp}(\phi)$ has eight-fold symmetry and vanishes at $\phi = \frac{n\pi}{4}$, $n = 0, 1, \dots, 7$.

A number of experiments on the cuprates suggest that the scattering rate has a four-fold variation around the Fermi surface. Such variations are also seen in calculations for a doped Hubbard model, using Cellular Dynamical Mean-Field theory.³¹ A simple hot or cold spots model of scattering^{32,33} yields

$$\frac{1}{\tau(\phi)} = \frac{1}{\tau_0} (1 + \alpha \cos(4\phi)), \quad (23)$$

where $\alpha > 0$ for cold spots located at $\phi = \pm \frac{\pi}{2}, \pm \frac{3\pi}{2}$. We parametrize the anisotropy in the FS and the cyclotron frequency as:

$$k_F(\phi) = k_F^0 (1 + \kappa \cos(4\phi)), \quad (24)$$

$$\frac{1}{\omega_0(\phi)} = \frac{1}{\omega_{00}} (1 + u \cos(4\phi)). \quad (25)$$

In Fig. 3 we show the effects of adding various anisotropies to the calculated AMRO. In Fig. 3a we show the calculated AMRO only allowing for anisotropic interlayer hopping. This demonstrates that much of the overall form of the magnetoresistance curves is determined by the presence of the eight nodes in the interlayer hopping [Eq. (22)]. Due to this symmetry we only display AMRO for $\varphi \in [0, \frac{\pi}{4}]$. In Fig. 3b we add the effects of an anisotropic k_F which can be seen to depress $\rho_c(\theta)$ for small φ at large θ and enhance $\rho_c(\theta)$ for larger φ (up to $\frac{\pi}{4}$) at large θ . In Fig. 3c we make our fit self-consistent by also allowing for anisotropy in ω_0 , which tends to reduce $\rho_c(\theta)$ at larger θ for larger φ . When we also include scattering anisotropy, we recover the fit that we displayed in Fig. 2 for the following set of parameters: $\eta_1 = 0.675$, $t_{\perp}^0 \simeq 13$ meV, $ck_F^0 = 8.64$, $\omega_{00}\tau_0 = 0.45$, $\kappa = -0.033$, $u = -0.08$, and $\alpha = 0.01$.

The effect of anisotropic scattering on the shape of the curves is most pronounced at large values of θ , and the height of the peak in $\rho_c(\theta)$ at $\theta \sim 40^\circ$, for $\varphi \sim 0^\circ$. We use a small value of α here to fit the data, but larger values tend to be required at higher temperatures.¹⁵ Increasing α also increases the value of $\rho(\theta = 0) = \rho_0$.

For the overdoped cuprate we consider, a tight-binding model for the intralayer bands has been fit to ARPES data for a sample of similar chemical composition.³⁴ We use this model as an independent check of the reliability of the values we obtain for k_F^0 , ω_0 , u , and κ . The tight-binding fit gives comparable values which increases confidence that the extraction of anisotropies from AMRO is robust.

Equation (9) is valid for both coherent and weakly incoherent transport between layers, except in a small region near $\theta = 90^\circ$. For coherent transport, but not for incoherent transport, there is a peak in the resistivity at $\theta = 90^\circ$ due to orbits on the $3d$ FS that do not exist if one can only define a $2d$ FS within the layers.^{7,16} A second definitive signature of coherent interlayer transport is

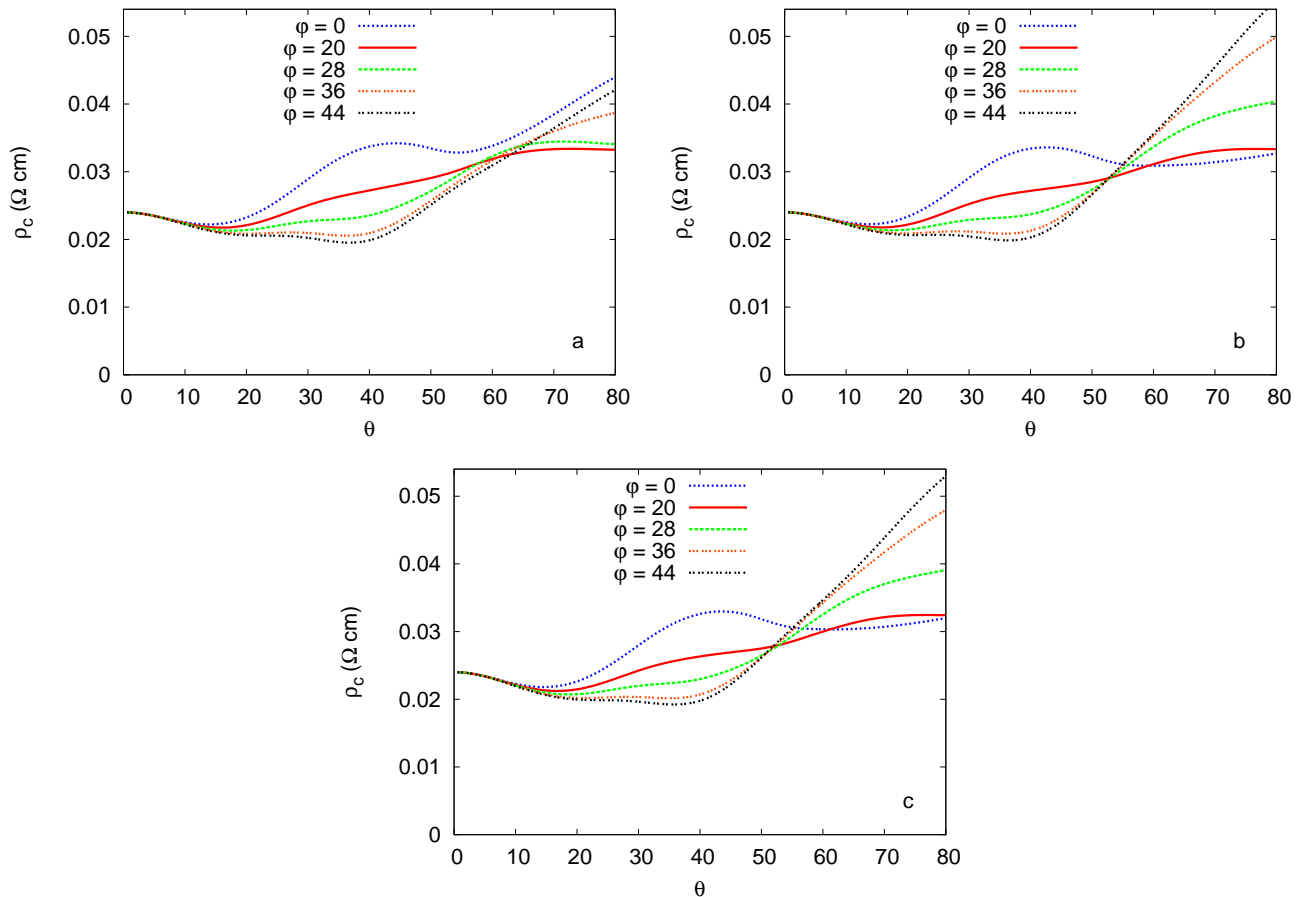


FIG. 3: Calculated angular dependence of the interlayer magnetoresistance for several different azimuthal angles, based on Eq. (9). For the parameter values used, $\eta_1 = 0.675$, $t_{\perp}^0 \simeq 13$ meV, $ck_F^0 = 8.64$, $\omega_{00}\tau_0 = 0.45$. In a) $\alpha = 0.0$, $\kappa = 0.0$, and $u = 0.0$, as defined in Eqs. (22) to (25). In b) we allow anisotropy in k_F , with $\kappa = -0.033$. In c) we allow anisotropy in k_F and ω_0 with $\kappa = -0.033$, and $u = -0.08$.

beats in quantum magnetic oscillations¹⁶ but these have not been seen in thallium cuprate. For the samples in Ref. 14, t_{\perp} and \hbar/τ_0 , are of the same order, which would place them at the boundary between coherent and incoherent interlayer transport. However, $\omega_{00}\tau_0$ is insufficiently large to be able to see either of these definitive signatures of coherence. This implies that further evidence is required to validate the claim of a 3d FS in Ref. 14, and so a 3d FS is *not* necessary to explain the AMRO data in Ref. 14.

V. DISCUSSION

In conclusion, we have given a general formula for AMRO in layered metals which have anisotropy in interlayer tunnelling, in intralayer scattering, and an anisotropic FS. We have performed explicit calculations for parameters relevant to experiments on thallium cuprate¹⁴ and shown that these do not on their own imply the coherence of interlayer transport. These fits are very sensitive to the anisotropies of intralayer properties.

Whilst we have focused our attention on the example of AMRO in thallium cuprate, our results have a much wider applicability – in fact to any layered metal with an anisotropic Fermi surface and anisotropic scattering. Our results have been stated for quasi-two-dimensional systems, but it should be fairly straightforward to generalize our results to quasi-one-dimensional systems such as Bechgaard salts, for which there is a substantial amount of AMRO data.^{7,8} We also discuss how AMRO can be used in conjunction with other techniques such as ARPES to place strong constraints on FS properties. Combined AMRO and ARPES studies of layered metals could give a strong consistency check for the results of both techniques and this suggests many future opportunities ahead for AMRO as a powerful probe of anisotropies in layered metals. In particular, for superconducting organic charge transfer salts a characterization of intralayer anisotropies, could reveal the presence of a pseudogap with d-wave symmetry, as predicted by a resonating valence bond theory of these materials.³⁵

Acknowledgments

We thank N. E. Hussey and M. Abdel-Jawad for stimulating discussions and for showing us unpublished ex-

perimental results. We thank B. J. Powell for a critical reading of the manuscript. This work was supported by the ARC (R.H.M.), and NSERC (M.P.K.). We thank Wolfson College, Oxford for hospitality.

-
- ¹ N. W. Ashcroft, and N. D. Mermin, “Solid State Physics”, Saunders (Philadelphia) (1976).
 - ² M. R. Norman, D. Pines, and C. Kallin, *Adv. Phys.* **54**, 715 (2005); P. A. Lee, N. Nagaosa, and X.-G. Wen, *Rev. Mod. Phys.* **78**, 17 (2006).
 - ³ A. J. Millis, *Nature* **417**, 599 (2002); T. Valla, P. D. Johnson, Z. Yusof, B. Wells, Q. Li, S. M. Loureiro, R. J. Cava, M. Mikami, Y. Mori, M. Yoshimura, and T. Sasaki, *Nature* **417**, 627 (2002).
 - ⁴ A. Damascelli, Z. Hussain, and Z.-X. Shen, *Rev. Mod. Phys.* **75**, 473 (2003).
 - ⁵ K. M. Shen, F. Ronning, D. H. Lu, F. Baumberger, N. J. C. Ingle, W. S. Lee, W. Meevasana, Y. Kohsaka, M. Azuma, M. Takano, H. Takagi, and Z.-X. Shen, *Science* **307**, 901 (2005).
 - ⁶ N. Mannella, W. L. Yang, X. J. Zhou, H. Zheng, J. F. Mitchell, J. Zaanen, T. P. Devereaux, N. Nagaosa, Z. Hussain, and Z.-X. Shen, *Nature* **438**, 474 (2005).
 - ⁷ M. V. Kartsovnik, *Chem. Rev.* **104**, 5737 (2004).
 - ⁸ J. Wosnitza, *Fermi Surfaces of Low Dimensional Organic Metals and Superconductors* (Springer Verlag, Berlin, 1996).
 - ⁹ L. Balicas, S. Nakatsuji, D. Hall, T. Ohnishi, Z. Fisk, Y. Maeno, and D. J. Singh, *Phys. Rev. Lett.* **95**, 196407 (2005).
 - ¹⁰ C. Bergemann, A.P. Mackenzie, S.R. Julian, D. Forsythe, and E. Ohmichi, *Adv. Phys.* **52**, 639 (2003).
 - ¹¹ T. Osada, H. Nose, and M. Kuraguchi, *Physica B* **294-295**, 402 (2001).
 - ¹² U. Beierlein, C. Schlenker, J. Dumas, and M. Greenblatt, *Phys. Rev. B* **67**, 235110 (2003).
 - ¹³ K. Enomoto, S. Uji, T. Yamaguchi, T. Terashima, T. Konoike, M. Nishimura, T. Enoki, M. Suzuki, and I. Suzuki, *Phys. Rev. B* **73**, 045115 (2006).
 - ¹⁴ N. E. Hussey, M. Abdel-Jawad, A. Carrington, A. P. Mackenzie, and L. Balicas, *Nature* **425**, 814 (2003).
 - ¹⁵ M. Abdel-Jawad, M. P. Kennett, L. Balicas, A. Carrington, A. P. Mackenzie, R. H. McKenzie, and N. E. Hussey, *Nature Physics* **2**, 821 (2006).
 - ¹⁶ R. H. McKenzie and P. Moses, *Phys. Rev. Lett.* **81**, 4492 (1998); P. Moses and R. H. McKenzie, *Phys. Rev. B* **60**, 7998 (1999).
 - ¹⁷ V. M. Yakovenko and B. K. Cooper, *Physica E* **34**, 128 (2006); B. K. Cooper and V. M. Yakovenko, *Phys. Rev. Lett.* **96**, 037001 (2006).
 - ¹⁸ D. Weiss, K. von Klitzing, K. Ploog, and G. Weimann, *Europhys. Lett.* **8**, 179 (1989).
 - ¹⁹ C. Beenakker, *Phys. Rev. Lett.* **62**, 2020 (1989).
 - ²⁰ J. P. Robinson, M. P. Kennett, N. R. Cooper, and V. I. Fal’ko, *Phys. Rev. Lett.* **93**, 036804 (2004); M. P. Kennett, J. P. Robinson, N. R. Cooper, and V. I. Fal’ko, *Phys. Rev. B* **71**, 195420 (2005).
 - ²¹ It is also worth noting that the derivation given here for weakly incoherent transport is actually simpler than that given previously for the more restrictive case of isotropic intralayer Fermi surface properties.¹⁶
 - ²² T. Osada, S. Kagoshima, and N. Miura, *Phys. Rev. B* **46**, 1812 (1992); A. G. Lebed and N. N. Bagmet, *Phys. Rev. B* **55**, 8654 (1997); L. N. Bulaevskii, M. J. Graf, and M. P. Maley, *Phys. Rev. Lett.* **83**, 388 (1999); Y. Oshima, M. Kimata, K. Kishigi, H. Ohta, K. Koyama, M. Motokawa, H. Nishikawa, K. Kikuchi, and I. Ikemoto, *Phys. Rev. B* **68**, 054526 (2003); R. Hlubina and B. Gheblawi, *phys. stat. sol. (b)* **225**, 115 (2001); A. E. Kovalev, S. Hill, K. Kawano, M. Tamura, T. Naito, and H. Kobayashi, *Phys. Rev. Lett.* **91**, 216402 (2003).
 - ²³ A. Drăgulescu, V. M. Yakovenko, and D. J. Singh, *Phys. Rev. B* **60**, 6312 (1999).
 - ²⁴ M. V. Kartsovnik, V.N. Laukhin, S.I. Pesotskii, I.F. Schegolev, and V.M. Yakovenko, *J. Phys. (France) I* **2**, 89 (1991).
 - ²⁵ V. G. Peschansky, J.A.R. Lopez, and T.G. Yao, *J. Phys. (France) I* **1**, 1469 (1991).
 - ²⁶ M. P. Kennett and R. H. McKenzie, unpublished.
 - ²⁷ Note that $t_{\perp}/E_F \sim 0.03$ for the sample in Ref. 14.
 - ²⁸ G. D. Mahan, “Many-Particle Physics”, second edition, Plenum (New York) (1993), p. 794.
 - ²⁹ I. L. Aleiner and A. I. Larkin, *Phys. Rev. B* **54**, 14423 (1996); A. M. Rudin, I. L. Aleiner, and L. I. Glazman, *Phys. Rev. B*, **58**, 15698 (1998).
 - ³⁰ D. van der Marel, *Phys. Rev. B* **60**, R765 (1999); T.M. Mishonov and M. Stoev, cond-mat/0504290.
 - ³¹ See for example, M. Civelli, M. Capone, S. S. Kancharla, O. Parcollet, and G. Kotliar, *Phys. Rev. Lett.* **95**, 106402 (2005).
 - ³² L. B. Ioffe and A. J. Millis, *Phys. Rev. B* **58**, 11631 (1998).
 - ³³ K. G. Sandeman and A. J. Schofield, *Phys. Rev. B* **63**, 094510 (2001).
 - ³⁴ M. Platé, J. D. F. Mottershead, I. S. Elfimov, D. C. Peets, R. X. Liang, D. A. Bonn, W. N. Hardy, S. Chiuzaian, M. Falub, M. Shi, L. Patthey, and A. Damascelli, *Phys. Rev. Lett.* **95**, 077001 (2005); D.C. Peets, J. D. F. Mottershead, B. Wu, I. S. Elfimov, R. X. Liang, W. N. Hardy, D. A. Bonn, M. Raudsepp, N. J. C. Ingle, and A. Damascelli, *New J. Phys.* **9**, 28 (2007).
 - ³⁵ B. J. Powell and R. H. McKenzie, *Phys. Rev. Lett.* **94**, 047004 (2005).